Comparison of Enzymes Immobilised on Immobeads and Inclusion Bodies
A Case Study of a Trehalose Transferase

Mestrom, Luuk; Marsden, Stefan R.; McMillan, Duncan G.G.; Schoevaart, Rob; Hagedoorn, Peter Leon; Hanefeld, Ulf

DOI
10.1002/cctc.202000241

Publication date
2020

Document Version
Final published version

Published in
ChemCatChem

doi.org/10.1002/cctc.202000241

Comparison of Enzymes Immobilised on Immobeads and Inclusion Bodies: A Case Study of a Trehalose Transferase

Luuk Mestrom,[a] Stefan R. Marsden,[a] Duncan G. G. McMillan,[a] Rob Schoevaart,[b] Peter-Leon Hagedoorn,[a] and Ulf Hanefeld*[a]

In this case study, we compare the performance of an enzyme immobilised using two different methods: i) as carrier-free catalytically active inclusion bodies or ii) as carrier-attached immobilised enzyme. To make this comparison we used a trehalose transferase from *Thermoproteus uzoniensis* fused to the fluorescent thermostable protein mCherry. The fusion of mCherry to trehalose transferase allowed direct spectrophotometric quantification and visualisation of the enzyme in both native and denatured states. The catalytically active inclusion bodies outperformed the immobilised enzyme in their simplicity of biocatalyst production resulting in high enzyme productivity. Enzyme immobilised on carrier materials showed a higher catalytic activity and a more robust performance under batch process conditions.

1. Introduction

Successful application of enzymes for the production of complex food products and chemicals depends on the recyclability of the biocatalyst and its ease of separation.[1] Enzyme immobilisation is a popular strategy for enzyme recycling and improvement of downstream processing. Since different enzyme immobilisation procedures influence the stability, activity, and selectivity of biocatalysts, a wide number of different methodologies have been developed.[2] The use of either carrier-free aggregates or carrier-attached enzymes are two of the most common techniques of enzyme immobilisation (Figure 1).[3] Catalytically active inclusion bodies (CatIBs) have been described as new form of carrier-free immobilisation[4] which has been successful for different enzyme classes,[5] such as hydrolases,[6] oxidoreductase,[7] lyases,[8] and transferases.[9] The simplicity of chromatography-free production and purification of CatIBs has been attributed the be the key to their success.[8]

To our knowledge, a direct comparison of enzymatic catalytic performance using the same enzyme as carrier-attached or carrier-free biocatalytic formulation has not been performed yet. One of the challenges in such a comparison is the characterisation of carrier-free CatIBs and their material properties. A high polydispersity in size and morphology of CatIBs complicates the analysis of diffusion limitation and the effect on catalytic activity within these particles. The CatIBs particles contain (partially) misfolded protein[10] possibly resulting in lower catalytic activity, independent of mass transfer limitations. The use of soft CatIBs can be disadvantageous, as continuous processes in a packed-bed plug flow reactor setup leads to pressure drops with compressible materials. It is not surprising that typically (fed-)batch processes have been reported with CatIBs.[5] Additional formulation steps are required to engineer the mechanical properties of CatIBs to broaden the choice of reactors.[11] In contrast, for carrier-attached enzymes the choice of reactor and the carriers dictate the material properties of the immobilisation matrix. Depending on the properties of the carrier, they can be used for different reactor types. A case by case optimisation of enzyme immobilisation with different attachment modes of carriers are required to guarantee optimal enzyme stability and activity.[12]

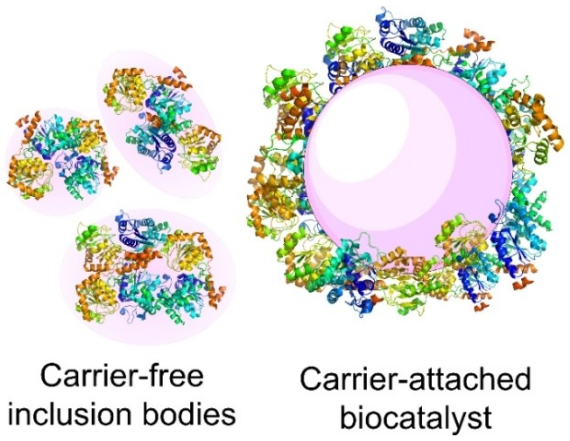

Figure 1. Schematic depiction of carrier-free CatIBs and carrier-attached attachment of enzyme.

Despite the plethora of enzyme immobilisation methodologies, including their optimisation strategies to increase their performance,[13] it remains challenging to assess the reduction in catalytic activity of immobilised enzymes. The immobilisation

[a] L. Mestrom, S. R. Marsden, Dr. D. G. G. McMillan, Dr. P.-L. Hagedoorn, Prof. U. Hanefeld
Biokatalyse, Afdeling Biotechnologie
Technische Universiteit Delft
Van Der Maasweg 9
2629 HZ Delft (The Netherlands)
E-mail: U.Hanefeld@tudelft.nl
[b] Dr. R. Schoevaart
ChiralVision
Hoog-Harnasch 44
2635 DL Den Hoorn (The Netherlands)
E-mail: Info@ChiralVision.com

Supporting information for this article is available on the WWW under https://doi.org/10.1002/cctc.202000241

procedure for attaching enzymes to carriers might affect the stability, activity, selectivity, and can influence the apparent inhibition.[14] Therefore well-characterised, commercial carriers were utilised in this study. The screening conditions were kept similar according to a standard immobilisation protocol. Different binding interactions can lead to (partial) protein denaturation, and enzymes can be distributed inhomogenously within an immobilisation matrix. The use of fluorescent proteins provides insight in these aspects during enzyme immobilisation. The enzyme used in this study, trehalose transferase from *Thermoproteus uzoniensis* (*Tu*TreT), was fused to fluorescent protein mCherry.[15] *Tu*TreT couples a nucleotide sugar donor and sugar acceptor in a (1→1)-α,α-glycosidic bond resulting in the formation of trehalose.[15] Although TreT has been applied for the synthesis of trehalose and its analogues,[16] TreT has been proven difficult to express as soluble enzyme.[15,17] The fusion of mCherry to *Tu*TreT resulted in increased solubility although still a large part of the expressed protein was in the form of CatIBs.[15] Upon denaturation of mCherry *Tu*TreT, the chromophore of mCherry changes colour from purple to green.[7a,18] Using the two different excitation and emission spectra, the quantitative and qualitative assessment between native and denatured mCherry *Tu*TreT is possible.[15] The potential of visualising protein aggregation and the distribution of native and denatured protein with and without carriers allow the evaluation of different protein immobilisation procedures.

The aim of this study was the comparison of the performance of a carrier-attached and carrier-free biocatalytic formulation of a single enzyme catalyst. The characterisation of the two biocatalytic formulations of mCherry *Tu*TreT was combined with essential parameters to measure the performance of each formulation: catalytic activity, operational stability, and ease of biocatalyst production. For the carrier-attached enzyme, twelve preexisting carriers with mCherry *Tu*TreT were explored with covalent, hydrophobic, or electrostatic interactions as attachment methodology (Table S1). The aim of this screening of carrier materials was to select the immobilised enzyme with the highest catalytic activity for further comparison. The CatIBs were extensively characterised, assessing the quality and quantity of mCherry *Tu*TreT and the effects of the binding interactions to various carriers. For both immobilisation techniques the fluorescent protein was used as a probe to assess the distribution and quality of the immobilised enzyme. The fusion of mCherry to *Tu*TreT allowed direct spectrophotometric quantification and visualisation of the enzyme in the native and denatured state. The CatIBs outperformed immobilised enzyme in their simplicity of biocatalyst production resulting in high enzyme productivity, while enzyme immobilised on carrier materials showed a higher catalytic activity and a more robust performance under batch process conditions.

2. Results and Discussion

To test the fluorescent protein mCherry to *Tu*TreT as a probe the immobilisation on twelve different commercial carriers was performed. All carriers were organic polymers with similar morphology, size, and porosity (material properties table S1). These carrier materials utilise different types of attachment interactions: covalent linkages using epoxide-functionalised polymers, absorption on hydrophobic materials, and electrostatic interactions with ionic carriers. mCherry *Tu*TreT was produced and purified as was described previously.[15] The progress of immobilisation was determined by visual inspection, since the intensity of purple colour of the immobilised enzyme and supernatant is proportional to the protein content.[15] Classification into 'high' (Figure 2a) and 'low' (Figure 2b) immobilisation efficiency was straightforward, and denaturation was readily identified by observing a change in colour from purple (folded mCherry) to green (denatured mCherry) (Figure 2c). With fluorescence microscopy three main states of immobilised *Tu*TreT fused to mCherry were observed: (i) uniform distribution on the surface without denaturation (Figure 2d); (ii) inhomogeneous distribution of native and denatured protein (Figure 2e); (iii) or the occurrence of fibrillar denatured protein aggregates on the surface of the carrier (Figure 2f).

The conventional characterisation of the immobilisation of enzymes on carriers relies on accurate protein quantification on the carrier material and the specific activity of the immobilised enzyme. Loss of specific enzyme activity upon immobilisation is often attributed to protein denaturation or diffusion limitation of the substrate. We performed this conventional characterisation together with fluorescence microscopy using mCherry as a reporter for the enzyme. 100 mg of enzyme carrier was added to 5.0 mg mCherry *Tu*TreT in 1.0 mL of HEPES buffer (50 mM, pH 7.0; see table S1). Both the activity and amount of any

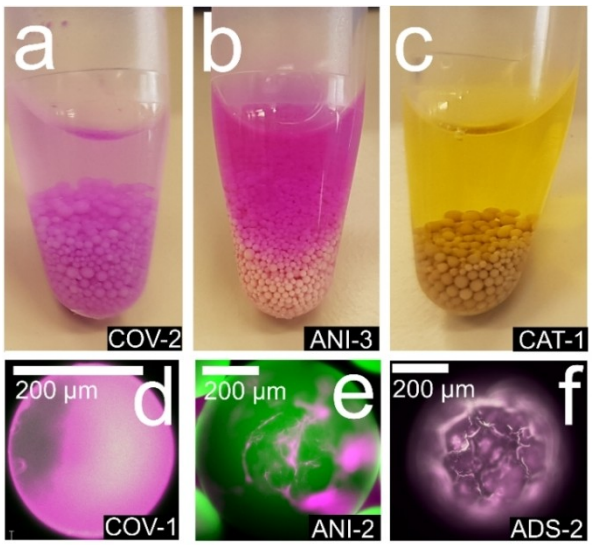

Figure 2. Visual inspection of the immobilisation procedure showing a high immobilisation yield of mCherry *Tu*TreT COV-2 (95% yield, 48 µg mg^{-1} carrier) in (**a**), moderate loading of ANI-3 in (**b**) (49%, 19 µg mg^{-1} carrier), and denatured mCherry *Tu*TreT on CAT-1 (**c**). Fluorescence microscopy of carrier-attached mCherry *Tu*TreT on COV-1 was homogenously distributed over the surface and inside the particles (**d**), where ANI-2 shows inhomogeneous distribution of native versus denatured enzyme (**e**). Aggregation of GFP-like fibrillar mCherry *Tu*TreT was observed on the surface of ADS-2 in (**f**).

remaining soluble enzyme was measured before and after immobilisation. mCherry *Tu*TreT is a monomer in solution,[15] and harbors 50 lysine residues per monomer (Figure S1) corresponding to 0.664 mmol of free amino groups per g of protein added to the carrier.

The highest immobilisation yields and specific activities of carrier-attached mCherry *Tu*TreT were found for immobilisation using covalent interactions (Figure 3a). Fluorescence microscopy showed a homogenous distribution of protein over the surface without protein denaturation (Figure S2). Lower catalytic activity and lower protein yields were observed after immobilisation using hydrophobic interactions (Figure 3b). Green fibrillar protein aggregates were observed on the hydrophobic surface of these carriers, suggesting that the lower catalytic activity observed was due to enzyme denaturation of the immobilised enzyme (Figure S3). This is in agreement with previous reports of protein aggregation or adverse folding effects using hydrophobic carriers.[2,19] For carriers with electrostatic attachment modes, the cationic carrier (CAT, Figure S4) showed complete denaturation of the protein without any recovery of the enzyme activity after immobilisation (Figure 3).

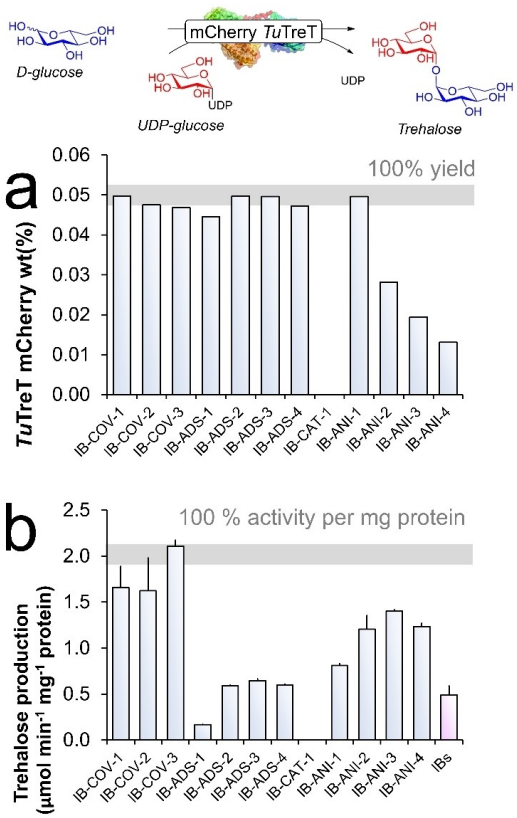

Figure 3. Immobilisation of mCherry *Tu*TreT on a wide range of carriers using either covalent (COV), hydrophobic (ADS), cationic (CAT), or anionic (ANI) binding modes. The immobilisation efficiency is high except for anionic binding modes (**a**), as was determined by relative decrease in protein content in solution ($\varepsilon_{587nm} = 0.9979\ mg^{-1} mL\ cm^{-1}$). The specific activity is highest for covalent binding modes (**b**), as was determined by measuring the activity per amount of protein on the carrier material. **Reaction conditions**: D-glucose (10 mM), UDP–D-glucose (40 mm), $MgCl_2$ (20 mM), HEPES (50 mM, pH 7.0).

The anionic carrier materials displayed an inhomogeneous distribution of native and denatured enzyme on the carrier materials (Figure S5). ATR-FTIR, widely used to measure the presence of proteins on the carriers, showed the characteristic amide I and II vibrations on the carriers, showing protein presence for all the carriers tested (Figure S6-S17).[20] Clearly the use of fluorescence microscopy showed more than just the presence of immobilized protein, as it yielded information on the native or denatured state of the protein and its distribution on the carrier material.

In light of the above described results, COV-1 was selected as the model system for the carrier-attached mCherry *Tu*TreT. The rate of immobilisation on different amounts of carrier material with a fixed amount of soluble mCherry *Tu*TreT ($1.0\ mg\ mL^{-1}$) was measured using spectroscopic UV-analysis (Figure S18). This characterisation allows the determination of the surface coverage of the spherical particles and the immobilisation process over time. Based on the ratio of amino groups (mCherry *Tu*TreT) to epoxide groups (COV-1), we determined the amount of accessible epoxide groups to be consistent with a surface coverage of approximately 40% (Figure S19).

The characterisation of carrier-free CatIBs as biocatalyst showed that mCherry could be used effectively as a reporter for the rapid analysis of both protein content and the state of denaturation of *Tu*TreT. This is particular useful in complex mixtures like inclusion bodies, since they are often contaminated with variable quantities of *E. coli* cell debris (i.e. other proteins).[8,21] When protein expression in *E. coli* is high, the mCherry *Tu*TreT inclusion bodies showed low amounts of contaminating proteins.[15] After separation from other cellular material, we took advantage of the sodium dodecyl sulphate (SDS) stability of *Tu*TreT and inclusion bodies were solubilised using 2% wt SDS.[15] The solubilised protein yield was then determined spectrophotometrically ($\varepsilon_{587\ nm} = 0.9979\ mg\ mL^{-1}\ cm^{-1}$) to correspond to 3% wt. mCherry *Tu*TreT in the CatIBs. Lyophilisation of the CatIBs allowed concentration of mCherry *Tu*TreT to 10% wt without loss of enzyme activity due to denaturation (Figure S20). Further analysis of the lyophilised CatIBs with ATR-FTIR showed characteristic amide I, II, III, and A vibrations which are typically observed for proteins (Figure 4a). Structural analysis with powder X-ray diffraction (XRD) of the CatIBs revealed the presence of (poorly) crystalline cross-β sheet interactions, with an interstrand distance of 4.7 Å and intersheet distance of 10 Å (Figure 4b-c). Similar cross β-sheet interaction distances have been reported for other IBs.[10] The hydrogen bonding of cross β-sheet interactions might be the major interaction governing the protein aggregation resulting in the carrier-free CatIBs. Fluorescence microscopy (Figure 4d-f, S21) revealed that mCherry *Tu*TreT contains mostly the native state within the CatIBs. Unfortunately, the physical size of CatIBs could not be determined due to their polydispersity.

The thermostability of mCherry *Tu*TreT in the soluble, carrier-attached (COV-1), and carrier-free CatIBs was investigated (Fig S22). After 2 hours of incubation in HEPES buffer (50 mM, pH 7.0) at 60 °C, 35% of enzyme activity was lost for the carrier attached enzyme. Minor loss of enzyme activity was

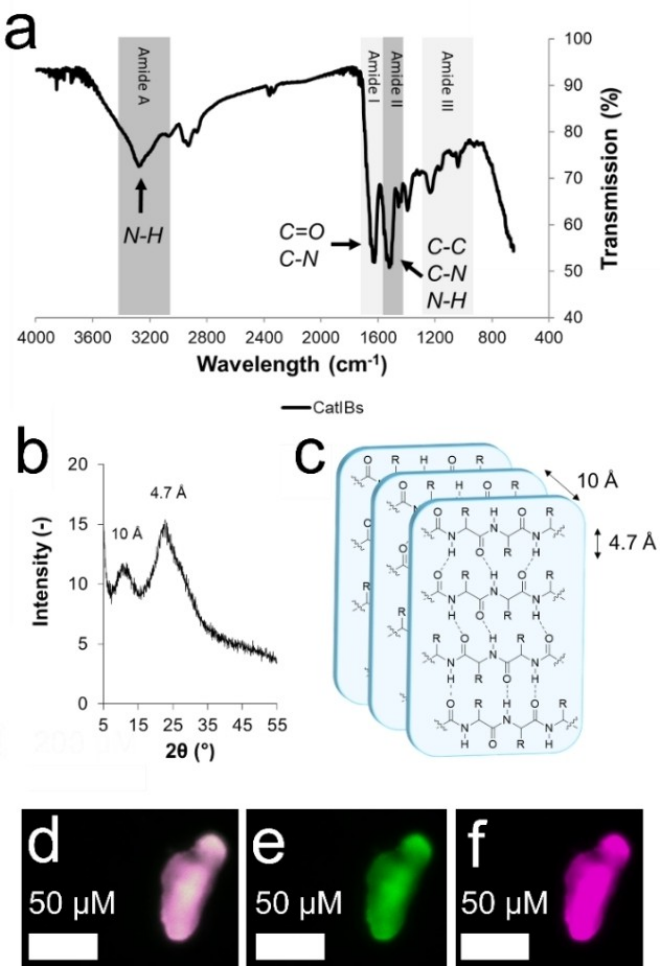

Figure 4. FTIR spectra of CatIBs of mCherry *Tu*TreT showing the distinctive amide A, I, II, and III vibrations (**a**). XRD analysis of cross-β interactions of mCherry *Tu*TreT CatIBs (**b**). The stacked β-sheets with an interstrand distance of 4.7 Å and intersheet distance of ~10 Å (R = amino acid residue) (**c**). Fluorescence microscopy of carrier-free CatIBs of mCherry *Tu*TreT showing the presence of denatured, GFP-like (green) and native (purple) mCherry protein (**d**). The GFP-like mCherry is measured with an excitation filter 488 nm-emission 522/35 nm (**e**) and for native mCherry an excitation filter of 568–585 nm (**f**) was used.

observed for the soluble form (0%) and CatIBs (5%) at 60 °C. The step-wise loss of enzyme activity from 70 °C to 80 °C was similar for soluble, carrier-free, and carrier-attached mCherry *Tu*TreT. At 90 °C, mCherry *Tu*TreT completely denatured. This was also evident from the loss of the purple colour. We hypothesise that the large loss of activity at 60 °C for the mCherry *Tu*TreT on COV-1 is due to the presence of unreacted epoxide groups. Upon heating at higher temperatures additional covalent linkages to mCherry *Tu*TreT can be formed, limiting structural mobility or causing the enzyme to denature. Enzyme deactivation when attached to epoxy functionalized carriers has been observed for multiple biocatalysts, where optimisation of their stability might be achieved by blocking agents or favouring multipoint covalent attachment.[22]

The recyclability of mCherry *Tu*TreT immobilised on a carrier or CatIBs is essential to maintain a high catalyst productivity in a batch process. The recyclability of enzyme on COV-1 before and after a heat-treatment was compared to CatIBs in ten consecutive cycles. Between each cycle, the biocatalyst was washed with buffer to remove the substrate and product. In line with the thermostability results, carrier-attached enzyme deactivated partially within the first 3 cycles at 60 °C (Figure 5). For the heat-treated carrier-attached mCherry *Tu*TreT, a stable performance during ten consecutive cycles was observed without leaching of any biocatalyst. The heat-treatment showed that the thermal deactivation happened only in the initial phase of the recycling due to the unreacted epoxide groups on the surface of the carrier, converging after a few cycles into similar conversion as samples that were not heat treated. The CatIBs showed no catalyst deactivation, which is consistent with the inactivation being linked to the carrier. The lower batch reproducibility of CatIBs arises from the difficulty to reproducibly resuspend the CatIBs after centrifugation. The sedimentation of the CatIBs particles typically lasted at least 5 minutes. To ensure optimal separation and no leaching of CatIBs, the solution was centrifuged at the end of each recycling step. This leads to differences in particle size distribution and therefore also a larger variation in catalytic activities, making it challenging to obtain a reproducible batch process with this procedure.

The next aspect of the comparison was the assessment of the catalytic performance of the immobilised enzymes. Both the enzyme activity during process conditions and the apparent kinetic parameters of the biocatalyst were investigated. During the biocatalytic operating process, the specific space-time yields (STY) per gram of catalyst or protein is higher for immobilised enzyme on COV-1 than for CatIBs, indicating that the carrier-immobilised mCherry *Tu*TreT demonstrates superior catalytic performance. The kinetic analysis of carrier-attached and carrier-free enzyme (table 1) gives the apparent catalytic turnover number ($k_{cat,\ app}$). This was 11-fold higher for carrier-attached enzyme than for the carrier-free CatIBs (Figure S23). Besides the catalytic activity, diffusion limitations due to the inaccessibility to the active site leads to a higher dissociation

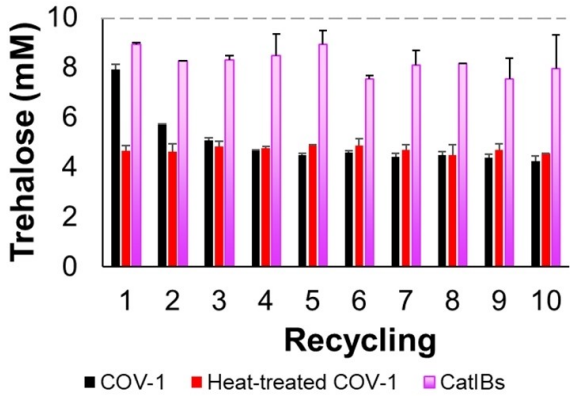

Figure 5. Recyclability of the immobilised mCherry *Tu*TreT COV-1 with or without heat-treatment (60 °C), or its inclusion bodies in batch operation. The dotted grey line indicates the maximum achievable conversion. **Reaction conditions**: Glucose (10 mM), UDP-glucose (40 mM), HEPES (50 mM, pH 7.5), $MgCl_2$ (20 mM), temperature 60 °C, 15 min reaction time.

Table 1. Comparing the performance of the biocatalytic formulation of carrier-attached mCherry *Tu*TreT to COV-1 or carrier-free CatIBs.

Name	Soluble	CatIBs	COV-1
Batch [nr]	1	10	10
Reaction volume [mL]	1	10×1=10	10×1=10
Reaction time [min]	30	10×15=150	10×15=150
Temperature [°C]	60	60	60
Conversion [% over nr batches]	100	82	50
Trehalose [mmol of all batches]	0.010	0.082	0.050
Trehalose [mg over number of batches]	3.42	28.1	17.11
Catalyst [mg catalyst mL^{-1}]	0.50	40	5.30
$k_{cat,\ app}$ [s^{-1}]	14±0.36[a]	0.49±0.10[b]	5.7±2.0[b]
$K_{M,\ app}$ [mM]	2.3±0.58[a]	10.3±3.2[b]	20.1±10.0[b]
$K_{I,\ app}$ [mM]	17±2.2[a]	17.2±5.2[b]	19.8±9.7[b]
STY [$g\,L^{-1}\,d^{-1}$]	164	135	82
STY [$g\,L^{-1}\,d^{-1}$] per g catalyst	n.a.[c]	3	15
STY [$g\,L^{-1}\,d^{-1}$] per g protein	327	130	329

[a] Ref. 15. [b] Reported $k_{cat,\ app}$, $K_{M,\ app}$, and $K_{I,\ app}$ are apparent kinetic parameters. [c] n.a.; not applicable.

constant of the immobilised catalyst. Indeed, the apparent $K_{M,\ app}$ and $K_{i,\ app}$ increased with the same order of magnitude for CatIBs and COV-1 in comparison to the soluble enzyme (Table 1). The catalytic performance the carrier-attached on COV-1 is significantly better for than carrier-free CatIBs.

The simplicity of production of the immobilised enzyme is one of the key contributors to a successful implementation in applied biocatalysis. In order to compare the amount of product produced of carrier-free or carrier-attached biocatalyst, the enzymatic productivity $g_{product}$ per amount of catalyst or bacterial culture was determined (Table S2). Due to the ease of protein production as insoluble CatIBs, the enzymatic productivity expressed as $g_{product}$ per liter of culture, is higher for CatIBs. Besides the increased protein production in the form of insoluble CatIBs, simple chromatography-free down-stream processing and the abolishment of additional contaminating material (i.e. unreacted monomers of polymeric carrier materials) is beneficial for potential pharmaceutical and food-grade applications. It is important to note that we have presented a methodology to evaluate the performance of one single CatIBs formulation, while the stability and enzymatic activity of other CatIBs can vary. For instance, different stabilities and activities have been reported when biocatalysts contained a fusion domain or peptide for tailor-made CatIBs.[5,23]

3. Conclusions

The soluble expression of biocatalysts can be challenging to achieve. The fusion of fluorescent protein mCherry offers rapid insight in different formulations of immobilised enzymes. We highlighted the use of the mCherry TreT fusion construct for monitoring the quality of the enzyme immobilised as CatIBs and as carrier attached immobilised enzymes. This allowed qualitative and quantitative assessment of native and denatured protein, and its distribution within an immobilisation matrix. The performance of CatIBs and immobilised enzymes were compared, revealing that CatIBs can be applied for batch reactions with high total productivity of trehalose per liter of expression host culture. Nevertheless, immobilised enzymes on carrier materials exhibit a superior catalytic performance and ease of separation. If enzyme solubility and expression can be increased, higher STY and catalytic efficiency can be achieved using enzymes immobilised on carriers. Taken together, these parameters show that carrier-attached enzymes are more suitable for large-scale batch reactions. A judicious choice between CatIBs or enzyme immobilisation for a particular batch process should be based on the required catalyst performance and the ease of enzyme production.

Experimental section

Materials

Ampicillin (Sigma-Aldrich), bovine serum albumin (ThermoFischer), DNAse I (bovine pancreas, Sigma-Aldrich), uridine 5′-diphosphate D-glucose disodium salt (Carbosynth, 98%), D-glucose (Sigma-Aldrich, 99.5%), HEPES (Sigma-Aldrich, >99.5%), formic acid (VWR), Mg(II)Cl_2 hexahydrate (VWR, >99.5%), tris(hydroxymethyl)aminomethane (Tris, 99%; Sigma-Aldrich), L-arabinose (Sigma-Aldrich, ≥99%), acetonitrile (ACN) (>99.5%; Sigma-Aldrich), Immobead kit (ChiralVision), acetone (Sigma-Aldrich).

The pH was adjusted with 0.014 △pKa/°C for HEPES buffer. Terrific broth medium consists of 1.20% (w/w) tryptone, 2.40% (w/w) yeast extract, 53 mM K_2HPO_4, 16 mM KH_2PO_4, 4% (w/w) glycerol, and autoclaved at 121 °C for 20 minutes.

Analytical equipment

Samples containing mCherry *Tu*TreT were analysed using an Axioplan 2 microscope (Zeiss, Mannheim, Germany), equipped with filterset XF108-2. Images were obtained using a Krypton/Argon laser using excitation 488 nm-emission 522/35 nm for denatured mCherry and excitation 568–585 nm long pass emission for mCherry. The projections of the individual channels were merged using the scientific image-analysis program ImageJ.[24] X-ray diffractometry (XRD) measurements were performed on a Bruker D8 Advance X-ray diffractometer using Co Ka radiation (1.78886 Å) at 35 kV and 40 mA equipped with a LynxEye detector. The data was collected from 5° to 80° 2 θ with a step size of 0.05° 2 θ and a counting time of 0.5 s per step. ATR-FTIR spectroscopy was performed with a Nicolet™ 6700 FT-IR spectrometer from Thermo Electron Corporation equipped with OMNIC Software, which were recorded at a wavenumber range from 4000–400 cm^{-1} (4 cm^{-1} resolution). UV-VIS spectroscopy was carried out with a Cary 60 UV-vis spectrophotometer (Agilent Technologies) connected to a Cary single cell Peltier accessory (Agilent Technologies). A laboratory alpha 2–4 Freeze Dryer (Christ) was used for lyophilisation of CatIBs of mCherry *Tu*TreT. All reactions were performed in an Eppendorf Thermomixer. Chromatographic analysis of reaction products was performed using a Shimadzu high-performance liquid chromatography (HPLC) system equipped with an Imtakt Unison-UK amino column (0.4 by 25 cm, 60 °C), an evaporative light-scattering detector (ELSD) (Shimadzu ELSD-LTII), a UV detector (SPD-20 A), and acetonitrile-water-formic acid at 80:20:0.1 as the mobile phase

(1 ml min^{-1}). The product formation was quantified using an external calibration curve, as is shown in Figure S24.

Protein homology model of mCherry *Tu*TreT

The protein crystal homology model was constructed using 4Q7 U[25] and 2XA9[26] for mCherry *Tu*TreT from the Protein Databank.[27] The surface potential was determined using the Adaptive Poisson-Boltzmann Solver plugin[28] in PyMOL Molecular Graphics system.[29]

Expression and purification of soluble and CatIBs of mCherry *Tu*TreT

The soluble protein and inclusion bodies of mCherry *Tu*TreT in *E. coli* Top10 pBAD/His A was expressed and purified as was described previously with minor changes.[15] The mCherry *Tu*TreT amino acid and DNA sequence is given in the supplementary information.

(i) Preparation of cell-free extract 5 mL precultures of *E. coli* Top10 pBAD/His A containing the mCherry *Tu*TreT genes were grown in LB-medium containing 100 μg mL^{-1} ampicillin at 37 °C overnight. To a 3 L baffled Fernbach flask containing 1 L TB-medium 20 mL preculture was added and induced by addition of L-arabinose to a final concentration of 0.02 % (w/w) after reaching an OD600 of 0.6–0.8. The cells were harvested after 14 hours by centrifugation (24515 g, 15 min, 4 °C) followed by resuspension of wet cell pellet in 4 mL lysis buffer containing Tris HCl buffer (50 mM, pH 8.0), imidazole (20 mM), lysozyme (0.5 mg mL^{-1}), DNaseI (0.1 mg mL^{-1}) per gram of wet cells. After 30 minutes of incubation on ice the cells were passed through the cell disruptor (1.35 kbar, Constant systems) for three consecutive rounds. The cell debris was collected via centrifugation 24515 g (Sorvall, Fiberlite F12-6x500 LEX, 10 min, 20 °C), and the CFE was obtained *via* decantation.

(ii) Immobilised nickel affinity chromatography The CFE was heat-treated at 60 °C for 20 minutes in a water bath. The precipitates were removed by centrifugation at 24515 g (Sorvall, Fiberlite F12-6x500 LEX, 10 min, 20 °C), and the heat-treated CFE was obtained via decanting. The heat-treated CFE was purified using affinity chromatography on a 1 mL Nickel Sepharose column by charging CFE on the column for at least three consecutive rounds using a peristaltic pump (Bio-Rad). The column was washed with binding buffer (20 mM Tris HCl, 500 mM NaCl, 20 mM imidazole, pH 8.0) until no protein eluted any longer. The attached mCherry *Tu*TreT was eluted using elution buffer (20 mM Tris HCl, 500 mM NaCl, 500 mM imidazole, pH 8.0) using a gradient over 10 column volumes. Protein samples were concentrated in a 12 mL Amicon Ultra Centrifugal filter (Merck, 30 kDa). Elution buffer was exchanged for HEPES (50 mM, pH 7.0) containing $MgCl_2$ (20 mM) by washing three consecutive rounds with 12 mL Amicon Ultra Centrifugal filters (Merck, 30 kDa), and analysed with SDS-PAGE and HPLC.

(iii) Purification of inclusion bodies The insoluble debris was homogenised in 20 mL Tris HCl buffer (50 mM, pH 8.5) containing 1 % (w/w) deoxycholic acid (DOC). The solubilised trehalose transferase was separated from the inclusion bodies via centrifugation (20 000 × *g*, 15 min, 20 °C). The resuspension and centrifugation were repeated twice. Subsequently, Tris HCl buffer (50 mM, pH 8.5) was utilised to remove remaining DOC in the cell pellet. The inclusion bodies were harvested *via* centrifugation (20 000 × *g*, 15 min, 20 °C). The supernatant was decanted, resulting in the isolation of wet inclusion bodies. The wet inclusion bodies were frozen at −80 °C. The purity with SDS-PAGE has been reported previously.[15] More details are shown in Table S2.

Lyophilisation mCherry *Tu*TreT CatIBs

The frozen wet inclusion bodies of mChery *Tu*TreT (−80 °C) were lyophilised (0.05 mbar, −72 °C) within 12 hours. The resulting weight loss of 62 % (w/w) a dry, purple powder was obtained. The lyophilised powder and wet inclusion bodies were solubilised in 2 % SDS in Tris-HCl buffer (50 mM, pH 8.0) and protein content was measured spectrophotometrically (λ_{587nm} = 0.9979 mL mg^{-1} cm^{-1}). The concentration of mCherry *Tu*TreT of wet CatIBs increased from 3 % wt to 10 % wt for the dry CatIBs. The protein did not denature with a GFP-like absorbance (Figure S20). The dry mCherry *Tu*TreT CatIBs were stored at −20 °C in the dark and the activity was determined with HPLC. The 1.5 mL polypropylene Eppendorf vial containing 1.0 mL reagent mixture of D-glucose (10 mM), UDP–D-glucose (40 mM), HEPES (50 mM, pH 7.0), and $MgCl_2$ (20 mM) with either wet or freeze-dried mCherry *Tu*TreT IBs. The reaction was started and stirred at 1400 rpm at 60 °C. After 15 minutes 100 μL of sample was quenched by the addition of 100 μL ice-cold HPLC-grade acetonitrile:water:formic acid (80 : 20:0.1) and incubated at −80 °C for one hour. The samples were centrifuged at 24515 g for 10 min at 4 °C. The supernatant was collected and analysed by HPLC (column: Imtakt UK-Amino 250 × 4.6 mm, 50 °C, ELSD, 80 : 20:0.1 acetonitrile:water:formic acid, 1.0 mL min^{-1}).

Protein quantification

Protein was quantified according to a method reported earlier, using the mass extinction coefficient of mCherry *Tu*TreT (ε_{587nm} = 0.9979 mg^{-1} mL cm^{-1}).[15] A protocol for the solubilisation of inclusion bodies in 2 % SDS in Tris-HCl buffer (50 mM, pH 8.0) was utilised, as has been reported earlier.[15,30]

Screening of Immobeads with mCherry *Tu*TreT

To 100.0 mg of carrier material 1.196 mL mCherry *Tu*TreT (5.0 mg, 4.18 mg mL^{-1} protein, 40 U) in HEPES buffer (50 mM, pH 7.0) was added and incubated overnight (4 °C, 10 rpm, NeoLab rotator). The supernatant was transferred and residual protein content was measured spectrophotometrically (λ_{587nm} = 0.9979 mL mg^{-1} cm^{-1}). The immobilised enzymes were filtered and washed with 1 mL ice-cold MiliQ water. The immobilised enzymes were washed with ice-cold acetone, filtered, and dried with air. The activity of the immobilised enzymes was determined using a HPLC-based activity assay. A 1.5 mL polypropylene Eppendorf tube containing 1.0 mL reagent mixture of D-glucose (10 mM), UDP–D-glucose (40 mM), HEPES (50 mM, pH 7.0), and $MgCl_2$ (20 mM) with 5 mg carrier material containing immobilised mCherry *Tu*TreT (max 2 U of soluble enzyme activity immobilised, maximum 0.25 mg of soluble protein) and stirred at 1400 rpm at 60 °C. After one hour of reaction time, 100 μL samples were quenched by the addition of 100 μL of reaction solution to an equal volume of ice-cold HPLC-grade acetonitrile:water:formic acid (80 : 20:0.1). The samples were centrifuged at 14 000 rpm for 10 min at 4 °C. The supernatant was collected and analysed by HPLC (column: Imtakt UK-Amino 250 × 4.6 mm, 50 °C, ELSD, 80 : 20:0.1 acetonitrile:water:formic acid, 1.0 mL min^{-1}). Enzyme activity was calculated with external standards for trehalose using the slope of at least three different substrate concentrations. The enzyme activity was determined in duplicate. One unit (U) is defined as the conversion of 1 μmol of D-glucose per minute.

Rate and surface coverage of mCherry *Tu*TreT on COV-1

To a solution containing 1.0 mg mL^{-1} mCherry *Tu*TreT, $MgCl_2$ (20 mM), HEPES (50 mM, pH 7.0) were added 0, 1, 2, 5, 7.5, 10, 15,

20, and 25 mg of COV-1 material in a polystyrene cuvette (pathlength 1 cm) and shaken at 4 °C at 1000 rpm. The absorbance of mCherry *Tu*TreT (ε_{587nm}) were measured within a time-course of 22 hours, as is shown in Figure S17. The surface coverage was measured by the evaluation of unreacted amino groups of a fixed amount of enzyme (1.07 mg, 0.71 μmol amino groups) and a varying amount of epoxide groups (1.0–25.0 mg COV-1, 70 nmol epoxides mg^{-1} carrier) after 22 hours of reaction time (Figure S18).

Temperature stability of immobillised mCherry TuTreT and CatIBs

The 1.5 mL polypropylene Eppendorf vial containing 1.0 mL containing: (i) soluble mCherry *Tu*TreT (0.02 mg mL^{-1}), HEPES (50 mM, pH 7.0), $MgCl_2$ (20 mM); (ii) CatIBs mCherry *Tu*TreT (40.0 mg wet CatIBs, 1.04 mg mCherry *Tu*TreT protein), HEPES (50 mM, pH 7.0), $MgCl_2$ (20 mM); (iii) COV-1 mCherry *Tu*TreT (5 mg mCherry *Tu*TreT COV-1, 0.25 mg protein mCherry *Tu*TreT), HEPES (50 mM, pH 7.0), $MgCl_2$ (20 mM) were incubated at 60–90 °C, 800 rpm, 2 hours of incubation time. After this, the enzyme activity was assayed for UDP–D-glucose (40 mM), D-glucose (10 mM), HEPES (50 mM, pH 7.0), $MgCl_2$ (20 mM), 800 rpm, 60 °C. The reaction was started by the addition of the biocatalyst and stirred at 1400 rpm at 60 °C. Samples were quenched by the addition of 100 μL ice-cold HPLC-grade acetonitrile:water:formic acid (80 : 20:0.1) between 0 to 35 minutes and incubated at −80 °C for one hour. The samples were centrifuged at 24515 g for 10 min at 4 °C. The supernatant was collected and analysed by HPLC (column: Imtakt UK-Amino 250× 4.6 mm, 50 °C, ELSD, 80 : 20:0.1 acetonitrile:water:formic acid, 1.0 mL min^{-1}). Enzyme activity was calculated with external standards for trehalose using the slope of at least three different substrate concentrations. The enzyme activity was determined in duplicate.

Recyclability of CatIBs and immobilised mCherry *Tu*TreT

The 1.5 mL polypropylene Eppendorf vial containing 1.0 mL reagent mixture of D-glucose (10 mM), UDP–D-glucose (40 mM), HEPES (50 mM, pH 7.0), and $MgCl_2$ (20 mM) with either wet 40.0 mg of mCherry *Tu*TreT IBs (1.04 mg protein), 5.3 mg COV-1 mCherry *Tu*TreT (0.44 U, 0.25 mg protein), or 5.3 mg COV-1 mCherry *Tu*TreT (0.44 U, 0.25 mg protein) which was heat-treated for 2 hours (50 mM HEPES, 20 mM $MgCl_2$, pH 7.0, 60 °C) before use. The reaction was started and stirred at 1400 rpm at 60 °C. After 15 minutes 100 μL of sample was quenched by the addition of 100 μL ice-cold HPLC-grade acetonitrile:water:formic acid (80 : 20:0.1) and incubated at −80 °C for one hour. The samples were centrifuged at 24515 g for 10 min at 4 °C. The supernatant was collected and analysed by HPLC (column: Imtakt UK-Amino 250 x 4.6 mm, 50 °C, ELSD, 80 : 20:0.1 acetonitrile:water:formic acid, 1.0 mL min^{-1}). The IBs or COV-1 of mCherry *Tu*TreT were centrifuged (30 s, 24515 g, 4 °C), washed with 1.0 mL HEPES (50 mM, pH 7.0) containing $MgCl_2$ (20 mM), and centrifuged (30 s, 24515 g, 4 °C). Again, the IBs or COV-1 of mCherry *Tu*TreT were centrifuged (30 s, 24515 g, 4 °C), washed with 1.0 mL HEPES (50 mM, pH 7.0) containing $MgCl_2$ (20 mM), and centrifuged (30 s, 24515 g, 4 °C). The reaction was started again by the addition of the reagent mixture of D-glucose (10 mM), UDP–D-glucose (40 mM), HEPES (50 mM, pH 7.0), and $MgCl_2$ (20 mM) with a final reaction volume of 1.0 mL. The reaction-wash-reaction step was repeated until a total of ten cycles were performed.

Apparent enzyme kinetics of CatIBs and immobilised mCherry *Tu*TreT

The 1.5 mL polypropylene Eppendorf vial containing 1.0 mL reagent mixture of D-glucose (10 mM), UDP–D-glucose (40 mM), HEPES (50 mM, pH 7.0), and $MgCl_2$ (20 mM) with either 20.0 mg lyophilised mCherry *Tu*TreT IBs (0.39 U, 2 mg) or 5.0 mg COV-1 mCherry *Tu*TreT (0.44 U, 0.25 mg protein). The reaction was started and stirred at 1400 rpm at 60 °C. Samples were quenched by the addition of 100 μL ice-cold HPLC-grade acetonitrile:water:formic acid (80 : 20:0.1) between 0 to 35 minutes and incubated at −80 °C for one hour. The samples were centrifuged at 24515 g for 10 min at 4 °C. The supernatant was collected and analysed by HPLC (column: Imtakt UK-Amino 250×4.6 mm, 50 °C, ELSD, 80 : 20:0.1 acetonitrile:water: formic acid, 1.0 mL min^{-1}). Enzyme activity was calculated with external standards for trehalose using the slope of at least three different substrate concentrations. The enzyme activity was determined in duplicate. The data was fitted (Gnuplot 5.2) to the equation shown in Figure S23.

Quantification of D-trehalose with HPLC

Samples during activity assays were quenched by the addition of 100 μL of reaction solution to an equal volume of ice-cold HPLC-grade acetonitrile and incubated at −80 °C for one hour. The samples were centrifuged at 24515 g for 10 min at 4 °C. The supernatant was collected and analysed by HPLC (column: Imtakt UK-Amino 250 x 4.6 mm, 50 °C, ELSD, 80 : 20:0.1 acetonitrile:water: formic acid, 1.0 mL min^{-1}). Enzyme activity was calculated with external standards for trehalose using the slope of at least three different substrate concentrations. The enzyme activity was determined in duplicate.

Acknowledgements

This research was supported by grant ERA-IB-15-110 of the ERA-NET on Industrial Biotechnology. We would like to acknowledge Marc Stampraad and Hessel van der Eijk (Delft University of Technology) for their efforts in producing mCherry Tu*TreT in* E. coli *Top10. Ben Norder is kindly acknowledged for his assistance measuring X-Ray diffraction (XRD). Diego Doornbos is kindly acknowledged for his assistance with fluorescence microscopy. We would also like thank Isabel Bento for sharing the homology model of mCherry* Tu*TreT.*

Conflict of Interest

The authors declare no conflict of interest.

Keywords: catalytically active inclusion bodies · trehalose transferase · immobilisation · glycosyltransferase

[1] A. Basso, S. Serban, *Mol. Catal.* **2019**, *479*, 110607.
[2] a) U. Hanefeld, L. Cao, E. Magner, *Chem. Soc. Rev.* **2013**, *42*, 6211–6212; b) G. Torrelo, N. van Midden, R. Stloukal, U. Hanefeld, *ChemCatChem* **2014**, *6*, 1096–1102; c) L. Mestrom, M. Przypis, D. Kowalczykiewicz, A. Pollender, A. Kumpf, S. R. Marsden, I. Bento, A. B. Jarzębski, K. Szymańska, A. Chruściel, D. Tischler, R. Schoevaart, U. Hanefeld, P.-L. Hagedoorn, *Int. J. Mol. Sci.* **2019**, *20*, 5263.

[3] L. Cao, L. van Langen, R. A. Sheldon, *Curr. Opin. Biotech.* **2003**, *14*, 387–394.
[4] a) U. Krauss, V. D. Jäger, M. Diener, M. Pohl, K.-E. Jaeger, *J. Biotechnol.* **2017**, *258*, 136–147; b) B. Nidetzky, *Protein Aggregation in Bacteria*, **2014**, pp. 247–261.
[5] R. Kloss, T. Karmainski, V. D. Jäger, D. Hahn, A. Grünberger, M. Baumgart, U. Krauss, K.-E. Jaeger, W. Wiechert, M. Pohl, *Catal. Sci. Technol.* **2018**, *8*, 5816–5826.
[6] a) S. Li, K. Lin, H. Pang, Y. Wu, J. Xu, *Appl. Biochem. Biotechnol.* **2013**, *169*, 612–623; b) Q. Dong, X. Yan, M. Zheng, Z. Yang, *J. Biosci. Bioeng.* **2014**, *117*, 706–710; c) D. M. Worrall, N. H. Goss, *Aust. J. Biotechnol.* **1989**, *3*, 28–32; d) K. Tokatlidis, P. Dhurjati, J. Millet, P. Béguin, J.-P. Aubert, *FEBS Lett.* **1991**, *282*, 205–208.
[7] a) E. García-Fruitós, N. González-Montalbán, M. Morell, A. Vera, R. M. Ferraz, A. Arís, S. Ventura, A. Villaverde, *Microb. Cell Fact.* **2005**, *4*, 27; b) S.-Y. Park, S.-H. Park, S.-K. Choi, *Anal. Biochem.* **2012**, *426*, 63–65.
[8] R. Kloss, M. H. Limberg, U. Mackfeld, D. Hahn, A. Grünberger, V. D. Jäger, U. Krauss, M. Oldiges, M. Pohl, *Sci. Rep. UK* **2018**, *8*, 5856.
[9] A. S. Korovashkina, A. N. Rymko, S. V. Kvach, A. I. Zinchenko, *J. Biotechnol.* **2013**, *164*, 276–280.
[10] L. Wang, S. K. Maji, M. R. Sawaya, D. Eisenberg, R. Riek, *PLoS Biol.* **2008**, *6*, e195.
[11] J. Nahálka, A. Vikartovská, E. Hrabárová, *J. Biotechnol.* **2008**, *134*, 146–153.
[12] a) T. Jesionowski, J. Zdarta, B. Krajewska, *Adsorption* **2014**, *20*, 801–821; b) M. Hoarau, S. Badieyan, E. N. G. Marsh, *Org. Biomol. Chem.* **2017**, *15*, 9539–9551.
[13] a) R. C. Rodrigues, C. Ortiz, Á. Berenguer-Murcia, R. Torres, R. Fernández-Lafuente, *Chem. Soc. Rev.* **2013**, *42*, 6290–6307; b) J. C. S. D. Santos, O. Barbosa, C. Ortiz, A. Berenguer-Murcia, R. C. Rodrigues, R. Fernandez-Lafuente, *ChemCatChem* **2015**, *7*, 2413–2432; c) C. Garcia-Galan, Á. Berenguer-Murcia, R. Fernandez-Lafuente, R. C. Rodrigues, *Adv. Synth. Catal.* **2011**, *353*, 2885–2904.
[14] a) C. Mateo, J. M. Palomo, G. Fernandez-Lorente, J. M. Guisan, R. Fernandez-Lafuente, *Enzyme Microb. Technol.* **2007**, *40*, 1451–1463; b) C. Mateo, R. Monti, B. C. C. Pessela, M. Fuentes, R. Torres, J. Manuel Guisán, R. Fernández-Lafuente, *Biotechnol. Prog.* **2004**, *20*, 1259–1262; c) B. C. C. Pessela, C. Mateo, M. Fuentes, A. Vian, J. L. García, A. V. Carrascosa, J. M. Guisán, R. Fernández-Lafuente, *Enzyme Microb. Technol.* **2003**, *33*, 199–205.
[15] a) L. Mestrom, S. R. Marsden, M. Dieters, P. Achterberg, L. Stolk, I. Bento, U. Hanefeld, P.-L. Hagedoorn, *Appl. Environ. Microbiol.* **2019**, *85*, e00942-00919; b) L. Mestrom, S. R. Marsden, M. Dieters, P. Achterberg, L. Stolk, I. Bento, U. Hanefeld, P.-L. Hagedoorn, *Appl. Environ. Microbiol.* **2019**, *85*, e03084-03018.
[16] B. L. Urbanek, D. C. Wing, K. S. Haislop, C. J. Hamel, R. Kalscheuer, P. J. Woodruff, B. M. Swarts, *ChemBioChem* **2014**, *15*, 2066–2070.
[17] T. Kouril, M. Zaparty, J. Marrero, H. Brinkmann, B. Siebers, *Arch. Microbiol.* **2008**, *190*, 355–369.
[18] a) L. A. Gross, G. S. Baird, R. C. Hoffman, K. K. Baldridge, R. Y. Tsien, *PNAS* **2000**, *97*, 11990–11995; b) B. J. Bevis, B. S. Glick, *Nat. Biotechnol.* **2002**, *20*, 83–87; c) I. I. Shemiakina, G. V. Ermakova, P. J. Cranfill, M. A. Baird, R. A. Evans, E. A. Souslova, D. B. Staroverov, A. Y. Gorokhovatsky, E. V. Putintseva, T. V. Gorodnicheva, T. V. Chepurnykh, L. Strukova, S. Lukyanov, A. G. Zaraisky, M. W. Davidson, D. M. Chudakov, D. Shcherbo, *Nat. Commun.* **2012**, *3*, 1204.
[19] U. Hanefeld, L. Gardossi, E. Magner, *Chem. Soc. Rev.* **2009**, *38*, 453–468.
[20] J. Andrade, C. G. Pereira, J. C. D. Almeida Junior, C. C. R. Viana, L. N. D. O. Neves, P. H. F. D. Silva, M. J. V. Bell, V. D. C. D. Anjos, *LWT-Food Sci. Technol.* **2019**, *99*, 166–172.
[21] R. Kloss, M. H. Limberg, U. Mackfeld, D. Hahn, A. Grünberger, V. D. Jäger, U. Krauss, M. Oldiges, M. Pohl, *Sci. Rep.* **2018**, *8*, 5856.
[22] C. Mateo, O. Abian, R. Fernandez-Lafuente, J. M. Guisan, *Enzyme Microb. Technol.* **2000**, *26*, 509–515.
[23] a) J.-P. Arié, M. Miot, N. Sassoon, J.-M. Betton, *Mol. Microbiol.* **2006**, *62*, 427–437; b) M. Diener, B. Kopka, M. Pohl, K.-E. Jaeger, U. Krauss, *ChemCatChem* **2016**, *8*, 142–152.
[24] C. A. Schneider, W. S. Rasband, K. W. Eliceiri, *Nat. Methods* **2012**, *9*, 671–675.
[25] S. Pletnev, D. M. Shcherbakova, O. M. Subach, N. V. Pletneva, V. N. Malashkevich, S. C. Almo, Z. Dauter, V. V. Verkhusha, *PLoS One* **2014**, *9*, e99136.
[26] E.-J. Woo, S.-I. Ryu, H.-N. Song, T.-Y. Jung, S.-M. Yeon, H.-A. Lee, B. C. Park, K.-H. Park, S.-B. Lee, *J. Mol. Biol.* **2010**, *404*, 247–259.
[27] H. M. Berman, J. Westbrook, Z. Feng, G. Gilliland, T. N. Bhat, H. Weissig, I. N. Shindyalov, P. E. Bourne, *Nucleic Acids Res.* **2000**, *28*, 235–242.
[28] E. Jurrus, D. Engel, K. Star, K. Monson, J. Brandi, L. E. Felberg, D. H. Brookes, L. Wilson, J. Chen, K. Liles, M. Chun, P. Li, D. W. Gohara, T. Dolinsky, R. Konecny, D. R. Koes, J. E. Nielsen, T. Head-Gordon, W. Geng, R. Krasny, G.-W. Wei, M. J. Holst, J. A. McCammon, N. A. Baker, *Protein Sci.* **2018**, *27*, 112–128.
[29] W. L. DeLano, *CCP4 Newsletter On Protein Crystallography* **2002**, *40*, 82–92.
[30] A. Singh, V. Upadhyay, A. K. Panda, *Insoluble Proteins: Methods and Protocols* (Ed.: E. García-Fruitós), Springer New York, New York, NY, **2015**, pp. 283–291.

Manuscript received: February 12, 2020
Revised manuscript received: April 15, 2020
Accepted manuscript online: April 16, 2020
Version of record online: [redacted], [redacted]

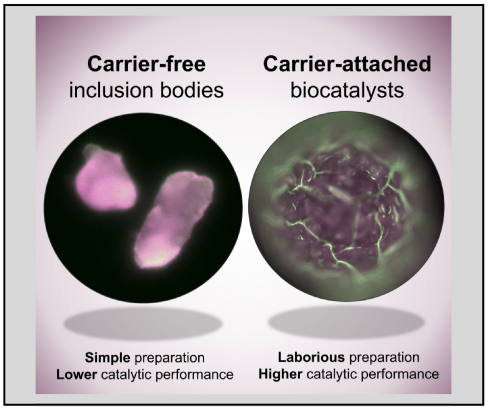

*L. Mestrom, S. R. Marsden, Dr. D. G. G. McMillan, Dr. R. Schoevaart, Dr. P.-L. Hagedoorn, Prof. U. Hanefeld**

Catalytically active inclusion bodies: In this case-study, immobilised trehalose transferase fused to mCherry was investigated in two distinct formulations: as inclusion bodies (left) and attached to a carrier (right). The use of mCherry as a fluorescent probe allows the visualisation of active (purple) *versus* inactive (green) biocatalyst, such as aggregation processes of enzymes.